Plasma Concentrations of Inflammatory Cytokines Rise Rapidly during ECMO-related SIRS due to the Release of Pre-formed Stores in the Intestine

Britt McILwain[1,2], **Joseph Timpa**[1], **Ashish R. Kurundkar**[3], **David W. Holt**[2], **David R. Kelly**[4], **Yolanda Hartman**[3], **Mary Lauren Neel**[3], **Rajendra K. Karnatak**[3], **Robert L. Schelonka**[5], **G. M. Anantharamaiah**[6], **Cheryl R. Killingsworth**[6], and **Akhil Maheshwari**[3,4,7]

[1] University Hospital Services, University of Alabama at Birmingham (UAB), Birmingham, AL

[3] Department of Pediatrics, UAB, Birmingham, AL

[4] Department of Pathology, UAB, Birmingham, AL

[6] Department of Medicine, UAB, Birmingham, AL

[7] Department of Cell Biology, UAB, Birmingham, AL

[5] Department of Pediatrics, Oregon Health and Science University, Portland, OR

[2] Clinical Perfusion Education, School of Allied Health Professions, University of Nebraska Medical Center, Omaha, NE

Abstract

Background—Extracorporeal membrane oxygenation (ECMO) is a life-saving support system used in neonates and young children with severe cardiorespiratory failure. Although ECMO has reduced mortality in these critically-ill patients, almost all patients treated with ECMO develop a systemic inflammatory response syndrome (SIRS) characterized by a 'cytokine storm', leukocyte activation, and multisystem organ dysfunction. We used a neonatal porcine model of ECMO to investigate whether rising plasma concentrations of inflammatory cytokines during ECMO reflect *de novo* synthesis of these mediators in inflamed tissues, and therefore, can be used to assess the severity of ECMO-related SIRS.

Methods—Three-week-old previously-healthy piglets were subjected to venoarterial ECMO for up to 8 hours. SIRS was assessed by histopathological analysis, measurement of neutrophil activation (flow cytometry), plasma cytokine concentrations (enzyme immunoassays), and tissue expression of inflammatory genes (polymerase chain reaction/western blots). Mast cell degranulation was investigated by measurement of plasma tryptase activity.

Results—Porcine neonatal ECMO was associated with systemic inflammatory changes similar to those seen in human neonates. TNF-α and interleukin-8 (IL-8) concentrations rose rapidly

---

during the first 2 hours of ECMO, faster than the tissue expression of these cytokines. ECMO was associated with increased plasma mast cell tryptase activity, indicating that increased plasma concentrations of inflammatory cytokines during ECMO may result from mast cell degranulation and associated release of preformed cytokines stored in mast cells.

Conclusions—TNF-α and IL-8 concentrations rose faster in plasma than in the peripheral tissues during ECMO, indicating that rising plasma levels of these cytokines immediately following the initiation of ECMO may not reflect increasing tissue synthesis of these cytokines. Mobilization of preformed cellular stores of inflammatory cytokines such as in mucosal mast cells may play an important pathophysiological role in ECMO-related SIRS.

Keywords

ECMO; venoarterial; neonate; SIRS; mast cells; intestine; CRP; cytokines

INTRODUCTION

Extracorporeal membrane oxygenation (ECMO) is used for providing cardiopulmonary support in critically-ill neonates and young children with respiratory failure, congenital heart disease, and overwhelming sepsis. While the availability of ECMO has reduced mortality in these patients by nearly 80%, concerns remain about the near-universal occurrence of a systemic inflammatory response syndrome (SIRS) during ECMO that is associated with multi-system organ dysfunction and considerable morbidity. This inflammatory response usually manifests within the first few hours of ECMO with hypotension, decreased urine output, decreased lung compliance, anasarca, and liver dysfunction, changes that frequently persist for several days and delay recovery from the underlying disease that led to ECMO in the first place (1–3). Elucidation of the mechanisms of ECMO-related SIRS is a critical step in the development of effective anti-inflammatory strategies, which may prevent adverse effects and thereby reduce the average duration of ECMO, encourage its institution earlier in the clinical course of cardiorespiratory failure rather than as a 'rescue' therapy of last resort, and possibly allow its application in a wider range of indications (1, 3).

ECMO-related inflammatory complications are more frequent in younger patients. Neonates and young infants are at greater risk because the enormous disparity between the patient's circulating blood volume and that of the circuit (circuit volumes are often 200–300% greater than patient's circulating blood volume) increases the activation of various blood components upon exposure to the foreign surface of the ECMO circuit (4, 5). The high incidence of ECMO-related complications in neonates is not altered by the configuration (veno-arterial vs. veno-venous) of ECMO or by the underlying cause of cardiorespiratory failure (6); developmental factors such as high metabolic demands, reactivity of the pulmonary vasculature, and immaturity of vascular autoregulation are believed to be more important (5). Our understanding of the inflammatory effects of extracorporeal circulation is based primarily on studies on adult patients treated with cardiopulmonary bypass (CPB) during cardiac surgery (7, 8). However, the extrapolation of data from CPB to ECMO is difficult because of major pathophysiological differences between the two modalities, such as the presence of defined ischemia-reperfusion sequences in CPB (related to the placement and release of aortic cross-clamps during cardiac surgery) but not in ECMO (9, 10).

In this study, we used a porcine neonatal model of ECMO to investigate the hypothesis that rising plasma concentrations of inflammatory cytokines during ECMO reflect *de novo* synthesis of these mediators in inflamed tissues, and therefore, can be used to assess the severity of ECMO-related SIRS. We subjected previously-healthy 3–6 kg piglets to venoarterial ECMO in the laboratory and detected inflammatory changes that were similar to those seen in human neonates. However, plasma concentrations of tumor necrosis factor-alpha (TNF-α) and interleukin-8 [IL-8, CXC-ligand 8 (CXCL8)] increased within the first two hours of ECMO, faster than the increase in tissue expression of these cytokines. These findings indicated that the increased plasma concentrations of inflammatory cytokines could not be completely explained on the basis of increased *de novo* synthesis in inflamed tissues and may have resulted, at least partially, from redistribution of preformed stores of these cytokines. Plasma TNF-α and IL-8 levels correlated with plasma mast cell tryptase activity, indicating that mast cell degranulation may contribute to the rapid rise of plasma cytokine concentrations during ECMO.

METHODS

Neonatal porcine ECMO

Animals—Mixed-breed neonatal piglets of either gender weighing 3–6 kg were subjected to venoarterial ECMO after approval by the UAB Institutional Animal Care and Use Committee. Sham animals received anesthesia, assisted ventilation, vascular cannulation, and heparinization similar to ECMO animals, but were not connected to the circulatory pump device. Data in this study represent 8 animals each in sham and ECMO groups; 3 animals in each group were euthanized after 2 hours of treatment and the remaining 5 after 8 hours.

Anesthesia, assisted ventilation and baseline support—The piglets were anesthetized with intramuscular atropine (0.04 mg/kg), tiletamine HCl/zolazepam HCl (4.4 mg/kg), and xylazine (4.4 mg/kg). All animals were intubated with a size 3.5 cuffed endotracheal tube and mechanically ventilated (volume controlled, tidal volume = 15 mL/kg, Hallowell EMC 2000 veterinary anesthesia ventilator) at a rate of 10–15 cycles/minute with the pig in a dorsally-recumbent position. Anesthesia was maintained by inhalation of isoflurane (1.5 to 2.5%) administered in 100% oxygen. Surface lead II EKG recordings, arterial blood pressure (ABP), and core (rectal) temperature was monitored. Water-heated pads were used to maintain normothermia (37 ± 1°C). Serum electrolyte levels and arterial blood gases were monitored throughout the study. Animals were given intravenous 0.9% saline at 2–5 mL/kg/hour during the experiment and also provided boluses as required to maintain normal ABP.

Vascular access—A multiple side-hole 8–10F Biomedicus venous cannula (Medtronic Perfusion Systems, Minneapolis, MN) was inserted into the external jugular vein and advanced into the right atrium. The common carotid artery was cannulated using a 6–8F Biomedicus arterial cannula. Placement of these cannulae was confirmed by fluoroscopy.

Heparinization—After circuit priming and before starting ECMO, animals were bolused with porcine heparin (Sigma, 150 U/kg), followed by additional intravenous heparin injections to maintain activated clotting times (ACT) of 180–220 seconds after initiation of ECMO.

ECMO procedure—ECMO circuit was primed with 1 liter 0.9% saline followed by 300 mL porcine whole blood collected from a similarly-anesthetized pig, 10 mL sodium bicarbonate, 1500 units of porcine heparin, and 50 mg calcium chloride. The venoarterial ECMO system consisted of a Biomedicus BP-50 centrifugal pump (Medtronic, Shoreview, MN), and a Minimax hollow fiber oxygenator (Medtronic) with an integral heat exchanger. Water bath temperatures were maintained at 37°C using a Sarns Dual Heater/Cooler (Soma Technology, Cheshire, CT). Gas flow rates to the membrane oxygenator were maintained at 0.5 L/min of 100% oxygen. After starting ECMO, the flow rates in the circuit were advanced to 350 mL/min or 1.5 L/min/m^2. Additional volume requirements to maintain circuit flow or desired hemoglobin level were met by the addition of a porcine whole blood or saline boluses. Animals were euthanized after 2 or 8 hours of ECMO by administration of potassium chloride.

Neutrophils

Neutrophils were isolated using an established density-centrifugation method (11). Briefly, porcine blood was mixed with 4% gelatin (Sigma, St. Louis, MO) in 0.9% NaCl and allowed to settle at 37°C for 30 min. The supernatant was then layered over Histopaque-1083 separation media (Sigma) and centrifuged at 400 *g* for 25 min at room temperature. Neutrophils were isolated from the resultant pellet after hypotonic lysis of the red blood cells and suspended in Hanks' balanced salt solution (HBSS; Sigma) (12). Cells were suspended in RPMI-1640 supplemented with 10% fetal bovine serum, and antibiotics.

Histopathological analysis and immunohistochemistry

Harvested tissues were fixed in formalin and embedded in paraffin. Histopathological examinations were performed on hematoxylin-eosin stained sections. Paraffin-embedded tissue sections were immunostained for c-kit (CD117, a mast cell marker), TNF-α, and IL-8/CXCL8 as described previously (12, 13). Briefly, tissue sections were deparaffinized with xylene and graded ethanols and antigen retrieval was achieved by heating the sections in 10 mM sodium citrate buffer, pH 6.0 at 95°C × 10 min followed by treatment with proteinase K (20 μg/mL; Sigma, St. Louis, MO) at 37°C × 20 minutes. After blocking overnight (Superblock, Pierce, Rockford, IL), the sections were stained overnight (4°C) with primary antibodies (mouse antibodies against c-kit and goat antibodies against TNF-α, and IL-8 from Santa Cruz Biotechnology, Santa Cruz, CA). Secondary staining was performed at room temperature for 30 min with Alexa 488- and/or Alexa 568-conjugated donkey anti-goat IgG and rabbit anti-mouse IgG (Invitrogen, San Diego, CA). Controls included slides with no primary antibody and appropriate isotype control. Cell nuclei were stained with 4′,6-diamidino-2-phenylindole (DAPI; Calbiochem, San Diego, CA), diluted 1:1000 in PBS, applied for 3 min. Imaging was performed using a fluorescence microscope (Carl Zeiss Microimaging, Inc., Thornwood, NY).

Flow cytometry

Neutrophils were stained for neutrophil activation markers CD18, CD35, CD62L, and CD11b using our previously-reported protocol (14). Controls included cells with no antibody and appropriate isotype control.

Real-time polymerase chain reaction

Real-time PCR was performed using our previously-described protocol (14). Total RNA was isolated using the acid guanidinium thiocyanate-phenol-chloroform extraction protocol (Trizol reagent, Invitrogen). First-strand cDNA was synthesized using oligo-dT primers and Moloney murine leukemia virus reverse transcriptase (Invitrogen). Real-time PCR primers were designed using the Beacon Design software (Bio-Rad, Hercules, CA). Two-step real-time PCR was performed using a SYBR Green protocol described elsewhere (14). Data were normalized against glyceraldehyde-3-phosphate dehydrogenase and gene expression was compared between samples by using the $2^{-\Delta\Delta CT}$ method.

Enzyme-linked immunosorbent assays

Plasma concentrations of porcine cytokines TNF-α, IL-8/CXCL8, IL-6, and IL-1β were measured by ELISA (R&D systems, Minneapolis, MA). ELISA kits for porcine CRP and C5a were purchased from Alpco Diagnostics, Salem, NH and Immunobiological Laboratories, Minneapolis, MN, respectively.

Western blots

Western blots were performed for TNF-α using our previously described protocol (14) and were analyzed using the NIH scion software.

Measurement of mast cell degranulation

We used a commercially-available assay (Millipore, Bedford, MA) based on the spectophotometric detection (405 nm) of a chromophore p-nitroaniline (pNA) released by tryptase action on a labeled substrate tosyl-gly-pro-lys-pNA.

Archived tissues from human neonates treated with ECMO

Autopsy samples from full-term human neonates who died during treatment with ECMO for pulmonary hypertension (n = 3) were obtained with approval of the local Institutional Review Board.

Statistical methods

Parametric and non-parametric tests were applied using the SigmaStat 3.1.1 software (Systat, Point Richmond, CA). The number of samples and the statistical analyses are described in figure legends. A p value of <0.05 was considered significant.

RESULTS

Hemodynamic changes during ECMO

The ECMO animals developed tachycardia and hypotension within 1–2 hours of initiation of ECMO. We treated hypotension with intravenous boluses of normal saline or porcine whole blood transfusions (given if hematocrit was <20%). In the ECMO group, capillary leakiness became clinically evident by about 4 hours of ECMO with abdominal distension due to ascites. Animals subjected to ECMO needed more frequent fluid boluses and blood transfusions (total administered volume 18 ± 9 mL/kg in sham animals vs. 178 ± 16 mL/kg in animals treated with ECMO, $p < 0.05$). The vital parameters of animals in sham and ECMO groups did not differ from each other.

Histopathological evidence of inflammation

Leukocyte infiltration, focal hemorrhages, and/or edema were evident in most tissues examined including the lung, intestine, liver, skin, and kidney after 2 hours of ECMO. These inflammatory changes increased in severity after 8 hours. These changes were most prominent in the lung and the intestine (Fig. 1A). These histopathological changes of inflammation in our porcine model were generally similar to changes noted in autopsy tissue samples from human neonates who died during ECMO (Fig. 1B). While the contribution of the underlying illness (that led to cardiopulmonary failure) to the inflammatory changes in these neonates cannot be clearly ascertained, these findings provide indirect evidence for our observations in the porcine model.

Neutrophil activation during ECMO

Because neutrophil activation is a key event during human ECMO (15, 16), we measured the expression of CD18, CD35, CD62L, and CD11b on circulating neutrophils in hourly samples from sham and ECMO animals by flow cytometry. Compared to sham animals, the expression of all four activation markers was significantly upregulated in ECMO animals. The expression of these markers at 2 hours (time point chosen to compare with histopathological changes of inflammation) is depicted in Fig. 1C.

Porcine ECMO was associated with a 'global' activation of pro-inflammatory genes

Using a real-time PCR microarray, we next measured mRNA expression of 48 well-characterized porcine inflammatory genes in lung and intestinal tissue. As shown in Fig. 2A, we detected increased expression of neutrophil chemokines IL-8/CXCL8 and growth-related oncoprotein-β/CXCL2 and mononuclear cell chemokines interferon-inducible protein-10/CXCL10, CXCL12, macrophage inflammatory protein-1β/CC-ligand 4, CCL11, and CCL21. Inflammatory cytokines such as TNF-α, interferon-γ, IL-1β, IL-6, IL-12, IL-15, and IL-18 were also upregulated. We also found increased tissue expression of the cognate receptors for TNF-α (TNF-receptor II), IL8 and GRO-β/CXCL2 (CXC receptors CXCR1 and CXCR2), CXCL10 (CXCR3), and MIP-1β/CCL4 (CCR3). The expression of nuclear factor-κB and activator protein 1 (AP-1) transcription factors was also increased. These changes showed that ECMO activated a wide range of pro-inflammatory genes encoding for

important chemokines, cytokines, cytokine/chemokine receptors, and critical transcriptional factors that regulate the expression of these cytokines and chemokines.

Increased plasma concentrations of pro-inflammatory cytokines

In support of data obtained from the PCR array shown in Fig. 4A, we compared the plasma concentrations of TNF-α, IL-8, IL-6, and IL-1β in sham and ECMO animals. We detected a rapid rise in plasma levels of TNF-α and IL-8 within the first two hours of ECMO, which was not observed in sham-treated animals (Fig. 2B). Plasma IL-1β and IL-6 levels increased more slowly, rising significantly after 4–6 hours of ECMO.

Onset of systemic inflammatory response during ECMO was not reflected in leukocyte counts or plasma CRP concentrations

We also investigated whether the onset of the systemic inflammatory response after initiation of ECMO was associated with changes in blood leukocyte counts or plasma CRP concentrations, two acute phase reactants that are frequently used in the clinical setting. Total leukocyte counts were $13.1 \pm 2 \times 10^9$/L and $12.4 \pm 3.2 \times 10^9$/L at 4 hours of treatment in sham vs. ECMO animals, respectively (differences not statistically significant). The absolute neutrophil counts were also not affected by ECMO ($8.9 \pm 1.2 \times 10^9$/L vs. $7.85 \pm 2.1 \times 10^9$/L in sham and ECMO animals, respectively). Similarly, plasma CRP concentrations were also not altered by ECMO-related SIRS (Fig. 3). Other acute phase reactants such as erythrocyte sedimentation rate and fibrinogen levels were considered but not evaluated during ECMO because of the presence of multiple confounding factors such as transfusions and heparinization.

Rapid rise in plasma TNF-α and IL-8 levels during ECMO is not matched by increased synthesis of these cytokines in the tissues

To investigate whether increased plasma concentrations of TNF-α and IL-8 during ECMO reflect increased *de novo* synthesis of these cytokines in inflamed tissues, we next measured mRNA and protein expression for TNF-α and IL-8 in tissues harvested from sham and ECMO animals after 2 hours of treatment. Although the mRNA expression of TNF-α increased in various tissues at 2 hours of ECMO (Fig. 4A), we did not detect important differences in TNF-α protein that could explain the rise in plasma TNF-α concentrations during ECMO at this time point. In contrast to the 8-fold increase in plasma TNF-α concentration at 2 hours of ECMO, TNF-α expression was decreased in the intestine and increased 1.5–2-fold in tissue samples from the liver and spleen (Fig. 4B). Similarly, we measured a 0.9–5-fold change in IL-8 mRNA in the tissues but the amount of IL-8 protein did not increase significantly in the tissues after 2 hours of ECMO; the expression of IL-8 was also decreased in the intestine at the 2 hour time-point (Supplemental Fig. 1).

Mast cells contain pre-formed TNF-α

Since the rapid rise in plasma TNF-α and IL-8 levels during ECMO could not be explained on the basis of increased *de novo* synthesis of these cytokines, we next investigated whether ECMO mobilized preformed tissue stores of TNF-α and IL-8 into the plasma. As seen in the western blots in Fig. 4B, the intestine contained the largest amounts of TNF-α in control

animals. These data were consistent with evidence that mast cells present in mucosal organs such as the intestine comprise the largest store of pre-formed TNF-α in the body (17, 18) and play an important role in experimental models of SIRS (19). In Fig. 4B, the reduction in TNF-α in the ECMO intestine was also consistent with the hypothesized release of cellular stores during ECMO. Therefore, we first used immunofluorescence microscopy to confirm whether porcine mucosal mast cells contained TNF-α. As seen in Fig. 5A, strong immunoreactivity for TNF-α was detected in c-kit^{+} mast cells in the intestine in both sham and ECMO animals. We also detected TNF-α in mast cells in sham/ECMO porcine lung, although the lung contained fewer mast cells than the intestine (not depicted). Mast cells also showed strong immunoreactivity for IL-8 in both sham and ECMO animals (not depicted). To confirm the pathophysiological relevance of mast cells in ECMO-related SIRS in human neonates, we also stained intestinal tissues from human neonates treated with ECMO (autopsy samples); a similar co-localization of c-kit and TNF-α was detected (Fig. 5B).

ECMO is associated with degranulation of mast cells

To investigate whether the initiation of ECMO in our porcine model was associated with mast cell degranulation, we next compared plasma samples from sham and ECMO animals for tryptase (mast cell protease 7) activity, a serine protease present almost exclusively and in large amounts in mast cell granules (20, 21). As shown in Fig. 5C, plasma tryptase activity after 1 hour of ECMO was nearly 4-fold higher than in sham animals and correlated with plasma concentrations of TNF-α and IL-8/CXCL8 ($p < 0.05$). Mast cell degranulation is a plausible event during ECMO because activation of the complement pathway in the membrane oxygenator releases several mast cell secretagogues such as C5a, C3a, and C3adesArg (22). Consistent with this hypothesis, we detected increased plasma C5a levels in our porcine model after 1 hour of ECMO (**inset,** Fig. 5C).

DISCUSSION

The histopathological changes of inflammation, activation of neutrophils, and increased plasma concentrations of various pro-inflammatory cytokines in our piglet model were generally similar to those reported in human ECMO (16, 23–25). Existing clinical and experimental evidence on the mechanisms of ECMO-related SIRS emphasizes the activation of neutrophils and other leukocytes as a pivotal event during ECMO, which occurs due to contact with the foreign surface of the circuit, shear stress, expression of inflammatory cytokines, activation of complement, coagulation and fibrinolytic pathways, and increased concentrations of bioactive lipids (16, 22–28). These activated neutrophils adhere to the capillary/venular endothelium and undergo degranulation to produce cytokines, arachidonic acid metabolites, and reactive oxygen species, causing widespread microvascular injury (15, 27) and multi-organ dysfunction (16, 22–28).

The rapid rise in plasma concentrations of TNF-α and IL-8 almost immediately after the initiation of ECMO suggests that these cytokines may be important mediators in the development of ECMO-related inflammation. TNF-α can induce the expression of a wide range of inflammatory genes, including its own (29), which suggests that the early rise in

circulating TNF-α levels during ECMO may form a 'feed-forward' loop to augment the inflammatory responses. In human neonates, higher plasma TNF-α concentrations have been noted in patients who died during ECMO than in 'responders' who recovered completely (16, 26, 30). In other studies, plasma concentrations of IL-8 correlated with the severity of SIRS and cardiopulmonary impairment during ECMO (16, 23, 24, 31).

The marked elevation in plasma cytokine levels in our model contrasted with the low sensitivity of acute phase reactants such as leukocyte counts and plasma CRP concentrations. Elevated CRP levels have been noted in one previous report on human ECMO (31) where CRP concentrations were higher in non-responders as compared to patients who improved on ECMO, although CRP was found to be less sensitive as a prognostic indicator than IL-6. The differential expression of IL-6 and CRP in our model was surprising because IL-6 is a potent inducer of CRP production in the liver and the two mediators are usually identified as bound variables in various inflammatory states (32). A possible explanation may be related to the 8-hour duration of our experiments, where we might have missed a late rise in plasma CRP concentrations (following the delayed rise in IL-6 levels). Alternatively, the CRP response may have been dampened by the relative resistance of porcine hepatocytes to IL-6, a species-specific feature. IL-6 induces CRP expression in hepatocytes via a CCAAT-enhancer-binding protein-beta (C/EBP-β)-mediated pathway (33), which carries unique posttranslational modifications and/or compartmentalization of C/EBP-β in pigs (34).

The increase in plasma TNF-α and IL-8 concentrations within 2 hours of initiation of ECMO in our model was not associated with a proportionate increase in the tissue synthesis of these cytokines at the same time. Considering the rapid change in plasma cytokine levels and also because the expression of TNF-α protein was actually decreased in the intestine at 2 hours, we hypothesized that ECMO mobilized these cytokines from preformed tissue stores of TNF-α into plasma. Of all the major cellular sources of TNF-α, mast cells (35) and eosinophils (36) are the only cell types considered capable of storing preformed TNF-α. We focused on mast cells and not eosinophils in this study because the gut mucosa normally contains a large reservoir of mast cells (17, 18). The plausibility of mast cell degranulation, as shown in our model, is supported by existing data on activation of complement and consequent release of mast cell secretagogues such as C5a, C3a, and C3adesArg during human ECMO (37). C3a levels have also been shown to correlate with plasma TNF-α levels and the severity of inflammation during ECMO (30).

Mast cells are now increasingly recognized as a major source of pre-formed TNF-α in SIRS in diverse settings such as in Gram-negative and Gram-positive bacterial sepsis, peritonitis, severe alveolar hypoxia, and portal hypertension (38–42). Unlike other major cellular sources of TNF-α such as macrophages and T-/B-lymphocytes that contain little or no detectable TNF-α unless appropriately stimulated (43, 44), mast cells present in mucosal organs contain large amounts of pre-formed TNF-α (17, 18) and play an important role in experimental models of SIRS (19). Histamine liberation has been previously reported during cardiopulmonary bypass (CPB) in older children and adults, but circulating basophils, and not mast cells, were incriminated as the source (45, 46). As we mentioned earlier, mechanistic differences in the inflammatory responses associated with ECMO vs. CPB are

not unexpected and illustrate the need for specifically-directed studies for these two forms of ECC. Even though ECMO and CPB are both performed using similar circulatory pumps and other major equipment, CPB is associated with several additional pathophysiological variables such as ischemia-reperfusion injury from aortic cross-clamping and due to the vasoconstrictive effects of hypothermia and hemodilution, pro-inflammatory effects of surgical trauma and tissue débris, and more frequent use of protamine (7, 8, 47–49).

In conclusion, the institution of ECMO in our porcine model induced systemic inflammatory changes that were remarkably similar to those reported during human ECMO. Although our original hypothesis that increased plasma TNF-α/IL-8 levels reflect tissue synthesis of these cytokines during ECMO was disproven, our data reaffirmed the higher sensitivity of inflammatory cytokines as indicators of inflammation during ECMO as compared to blood leukocyte counts and C-reactive protein. Further studies are needed to develop a panel of cytokines that are synthesized *de novo* during ECMO-related SIRS and not released from preformed stores. We have also identified mast cell degranulation and the release of TNF-α as early events in ECMO-related SIRS. The availability of agents that can stabilize enteric mast cells (50) as well as effective neutralizing anti-TNF-α antibodies raises important therapeutic possibilities (51) and indicates a need to aggressively investigate these targets in preclinical and clinical settings.

Supplementary Material

Refer to Web version on PubMed Central for supplementary material.

Acknowledgments

References

1. Kelly RE Jr, Phillips JD, Foglia RP, Bjerke HS, Barcliff LT, Petrus L, et al. Pulmonary edema and fluid mobilization as determinants of the duration of ECMO support. J Pediatr Surg. 1991; 26(9): 1016–1022. [PubMed: 1941476]

2. Ford JW. Neonatal ECMO: Current controversies and trends. Neonatal Netw. 2006; 25(4):229–238. [PubMed: 16913234]

3. Khoshbin E, Dux AE, Killer H, Sosnowski AW, Firmin RK, Peek GJ. A comparison of radiographic signs of pulmonary inflammation during ECMO between silicon and poly-methyl pentene oxygenators. Perfusion. 2007; 22(1):15–21. [PubMed: 17633130]

4. Butler J, Pathi VL, Paton RD, Logan RW, MacArthur KJ, Jamieson MP, et al. Acute-phase responses to cardiopulmonary bypass in children weighing less than 10 kilograms. Ann Thorac Surg. 1996; 62(2):538–542. [PubMed: 8694619]

5. Kozik DJ, Tweddell JS. Characterizing the inflammatory response to cardiopulmonary bypass in children. Ann Thorac Surg. 2006; 81(6):S2347–2354. [PubMed: 16731102]

6. Zahraa JN, Moler FW, Annich GM, Maxvold NJ, Bartlett RH, Custer JR. Venovenous versus venoarterial extracorporeal life support for pediatric respiratory failure: are there differences in survival and acute complications? Crit Care Med. 2000; 28(2):521–525. [PubMed: 10708194]

7. Ganapathy S, Murkin JM, Dobkowski W, Boyd D. Stress and inflammatory response after beating heart surgery versus conventional bypass surgery: the role of thoracic epidural anesthesia. Heart Surg Forum. 2001; 4(4):323–327. [PubMed: 11827861]

8. Brix-Christensen V. The systemic inflammatory response after cardiac surgery with cardiopulmonary bypass in children. Acta Anaesthesiol Scand. 2001; 45(6):671–679. [PubMed: 11421823]

9. Walker LK, Short BL, Traystman RJ. Impairment of cerebral autoregulation during venovenous extracorporeal membrane oxygenation in the newborn lamb. Crit Care Med. 1996; 24(12):2001–2006. [PubMed: 8968268]

10. Kuratani T, Matsuda H, Sawa Y, Kaneko M, Nakano S, Kawashima Y. Experimental study in a rabbit model of ischemia-reperfusion lung injury during cardiopulmonary bypass. J Thorac Cardiovasc Surg. 1992; 103(3):564–568. [PubMed: 1545556]

11. Stahl GL, Morse DS, Martin SL. Eicosanoid production from porcine neutrophils and platelets: differential production with various agonists. Am J Physiol. 1997; 272(6 Pt 1):C1821–1828. [PubMed: 9227410]

12. Maheshwari A, Kurundkar AR, Shaik SS, Kelly DR, Hartman Y, Zhang W, et al. Epithelial Cells in Fetal Intestine Produce Chemerin to Recruit Macrophages. Am J Physiol Gastrointest Liver Physiol. 2009

13. Smythies LE, Maheshwari A, Clements R, Eckhoff D, Novak L, Vu HL, et al. Mucosal IL-8 and TGF-beta recruit blood monocytes: evidence for cross-talk between the lamina propria stroma and myeloid cells. J Leukoc Biol. 2006; 80(3):492–499. [PubMed: 16793909]

14. Shaik SS, Soltau TD, Chaturvedi G, Totapally B, Hagood JS, Andrews WW, et al. Low-intensity shear stress increases endothelial ELR+ CXC chemokine production via a FAK-P38beta MAPK-NF-kappa B pathway. J Biol Chem. 2008

15. DePuydt LE, Schuit KE, Smith SD. Effect of extracorporeal membrane oxygenation on neutrophil function in neonates. Crit Care Med. 1993; 21(9):1324–1327. [PubMed: 8370296]

16. Fortenberry JD, Bhardwaj V, Niemer P, Cornish JD, Wright JA, Bland L. Neutrophil and cytokine activation with neonatal extracorporeal membrane oxygenation. J Pediatr. 1996; 128(5 Pt 1):670–678. [PubMed: 8627440]

17. Gordon JR, Galli SJ. Mast cells as a source of both preformed and immunologically inducible TNF-alpha/cachectin. Nature. 1990; 346(6281):274–276. [PubMed: 2374592]

18. Gordon JR, Galli SJ. Release of both preformed and newly synthesized tumor necrosis factor alpha (TNF-alpha)/cachectin by mouse mast cells stimulated via the Fc epsilon RI. A mechanism for the sustained action of mast cell-derived TNF-alpha during IgE-dependent biological responses. J Exp Med. 1991; 174(1):103–107. [PubMed: 1829107]

19. Tang C, Lan C, Wang C, Liu R. Amelioration of the development of multiple organ dysfunction syndrome by somatostatin via suppression of intestinal mucosal mast cells. Shock. 2005; 23(5):470–475. [PubMed: 15834315]

20. He S, Xie H. Modulation of tryptase and histamine release from human lung mast cells by protease inhibitors. Asian Pac J Allergy Immunol. 2004; 22(4):205–212. [PubMed: 15783133]

21. Shalit M, Schwartz LB, Golzar N, vonAllman C, Valenzano M, Fleekop P, et al. Release of histamine and tryptase in vivo after prolonged cutaneous challenge with allergen in humans. J Immunol. 1988; 141(3):821–826. [PubMed: 2456334]

22. Graulich J, Sonntag J, Marcinkowski M, Bauer K, Kossel H, Buhrer C, et al. Complement activation by in vivo neonatal and in vitro extracorporeal membrane oxygenation. Mediators Inflamm. 2002; 11(2):69–73. [PubMed: 12061426]

23. Underwood MJ, Pearson JA, Waggoner J, Lunec J, Firmin RK, Elliot MJ. Changes in "inflammatory" mediators and total body water during extra-corporeal membrane oxygenation (ECMO). A preliminary study. Int J Artif Organs. 1995; 18(10):627–632. [PubMed: 8647596]

24. Kawahito K, Misawa Y, Fuse K. Extracorporeal membrane oxygenation support and cytokines. Ann Thorac Surg. 1998; 65(4):1192–1193. [PubMed: 9564967]

25. Adrian K, Mellgren K, Skogby M, Friberg LG, Mellgren G, Wadenvik H. Cytokine release during long-term extracorporeal circulation in an experimental model. Artif Organs. 1998; 22(10):859–863. [PubMed: 9790084]

26. Mildner RJ, Taub N, Vyas JR, Killer HM, Firmin RK, Field DJ, et al. Cytokine imbalance in infants receiving extracorporeal membrane oxygenation for respiratory failure. Biol Neonate. 2005; 88(4):321–327. [PubMed: 16113527]

27. Graulich J, Walzog B, Marcinkowski M, Bauer K, Kossel H, Fuhrmann G, et al. Leukocyte and endothelial activation in a laboratory model of extracorporeal membrane oxygenation (ECMO). Pediatr Res. 2000; 48(5):679–684. [PubMed: 11044491]

28. Graves ED 3rd, Loe WA, Redmond CR, Falterman KW, Arensman RM. Extracorporeal membrane oxygenation as treatment of severe meconium aspiration syndrome. South Med J. 1989; 82(6): 696–698. [PubMed: 2734633]

29. Dempsey PW, Doyle SE, He JQ, Cheng G. The signaling adaptors and pathways activated by TNF superfamily. Cytokine Growth Factor Rev. 2003; 14(3–4):193–209. [PubMed: 12787559]

30. Plotz FB, van Oeveren W, Bartlett RH, Wildevuur CR. Blood activation during neonatal extracorporeal life support. J Thorac Cardiovasc Surg. 1993; 105(5):823–832. [PubMed: 7683735]

31. Risnes I, Wagner K, Ueland T, Mollnes T, Aukrust P, Svennevig J. Interleukin-6 may predict survival in extracorporeal membrane oxygenation treatment. Perfusion. 2008; 23(3):173–178. [PubMed: 19029268]

32. Herzum I, Renz H. Inflammatory markers in SIRS, sepsis and septic shock. Curr Med Chem. 2008; 15(6):581–587. [PubMed: 18336272]

33. Cha-Molstad H, Young DP, Kushner I, Samols D. The interaction of C-Rel with C/EBPbeta enhances C/EBPbeta binding to the C-reactive protein gene promoter. Mol Immunol. 2007; 44(11):2933–2942. [PubMed: 17335903]

34. Schrem H, Kleine M, Borlak J, Klempnauer J. Physiological incompatibilities of porcine hepatocytes for clinical liver support. Liver Transpl. 2006; 12(12):1832–1840. [PubMed: 17133583]

35. Gurish MF, Boyce JA. Mast cells: ontogeny, homing, and recruitment of a unique innate effector cell. J Allergy Clin Immunol. 2006; 117(6):1285–1291. [PubMed: 16750988]

36. Spencer LA, Szela CT, Perez SA, Kirchhoffer CL, Neves JS, Radke AL, et al. Human eosinophils constitutively express multiple Th1, Th2, and immunoregulatory cytokines that are secreted rapidly and differentially. J Leukoc Biol. 2009; 85(1):117–123. [PubMed: 18840671]

37. Hocker JR, Wellhausen SR, Ward RA, Simpson PM, Cook LN. Effect of extracorporeal membrane oxygenation on leukocyte function in neonates. Artif Organs. 1991; 15(1):23–28. [PubMed: 1998487]

38. Mallen-St Clair J, Pham CT, Villalta SA, Caughey GH, Wolters PJ. Mast cell dipeptidyl peptidase I mediates survival from sepsis. J Clin Invest. 2004; 113(4):628–634. [PubMed: 14966572]

39. Sutherland RE, Olsen JS, McKinstry A, Villalta SA, Wolters PJ. Mast cell IL-6 improves survival from Klebsiella pneumonia and sepsis by enhancing neutrophil killing. J Immunol. 2008; 181(8): 5598–5605. [PubMed: 18832718]

40. Nautiyal KM, McKellar H, Silverman AJ, Silver R. Mast cells are necessary for the hypothermic response to LPS-induced sepsis. Am J Physiol Regul Integr Comp Physiol. 2009; 296(3):R595–602. [PubMed: 19109365]

41. Chao J, Wood JG, Gonzalez NC. Alveolar hypoxia, alveolar macrophages, and systemic inflammation. Respir Res. 2009; 10(1):54. [PubMed: 19545431]

42. Tang CW, Lan C, Liu R. Increased activity of the intestinal mucosal mast cells in rats with multiple organ failure. Chin J Dig Dis. 2004; 5(2):81–86. [PubMed: 15612663]

43. Old LJ. Tumor necrosis factor (TNF). Science. 1985; 230(4726):630–632. [PubMed: 2413547]

44. Cuturi MC, Murphy M, Costa-Giomi MP, Weinmann R, Perussia B, Trinchieri G. Independent regulation of tumor necrosis factor and lymphotoxin production by human peripheral blood lymphocytes. J Exp Med. 1987; 165(6):1581–1594. [PubMed: 3108447]

45. Seghaye MC, Duchateau J, Grabitz RG, Mertes J, Marcus C, Buro K, et al. Histamine liberation related to cardiopulmonary bypass in children: possible relation to transient postoperative arrhythmias. J Thorac Cardiovasc Surg. 1996; 111(5):971–981. [PubMed: 8622322]

46. Withington DE, Aranda JV. Histamine release during cardiopulmonary bypass in neonates and infants. Can J Anaesth. 1997; 44(6):610–616. [PubMed: 9187780]

47. Yeh CH, Chen TP, Lee CH, Wu YC, Lin YM, Lin PJ. Cardioplegia-induced cardiac arrest under cardiopulmonary bypass decreased nitric oxide production which induced cardiomyocytic apoptosis via nuclear factor kappa B activation. Shock. 2007; 27(4):422–428. [PubMed: 17414426]

48. Asimakopoulos G. Systemic inflammation and cardiac surgery: an update. Perfusion. 2001; 16(5): 353–360. [PubMed: 11565890]

49. Ko WJ, Chen YS, Lee YC. Replacing cardiopulmonary bypass with extracorporeal membrane oxygenation in lung transplantation operations. Artif Organs. 2001; 25(8):607–612. [PubMed: 11531710]

50. Penissi AB, Rudolph MI, Villar M, Coll RC, Fogal TH, Piezzi RS. Effect of dehydroleucodine on histamine and serotonin release from mast cells in the isolated mouse jejunum. Inflamm Res. 2003; 52(5):199–205. [PubMed: 12813624]

51. Choo-Kang BS, Hutchison S, Nickdel MB, Bundick RV, Leishman AJ, Brewer JM, et al. TNF-blocking therapies: an alternative mode of action? Trends Immunol. 2005; 26(10):518–522. [PubMed: 16087401]
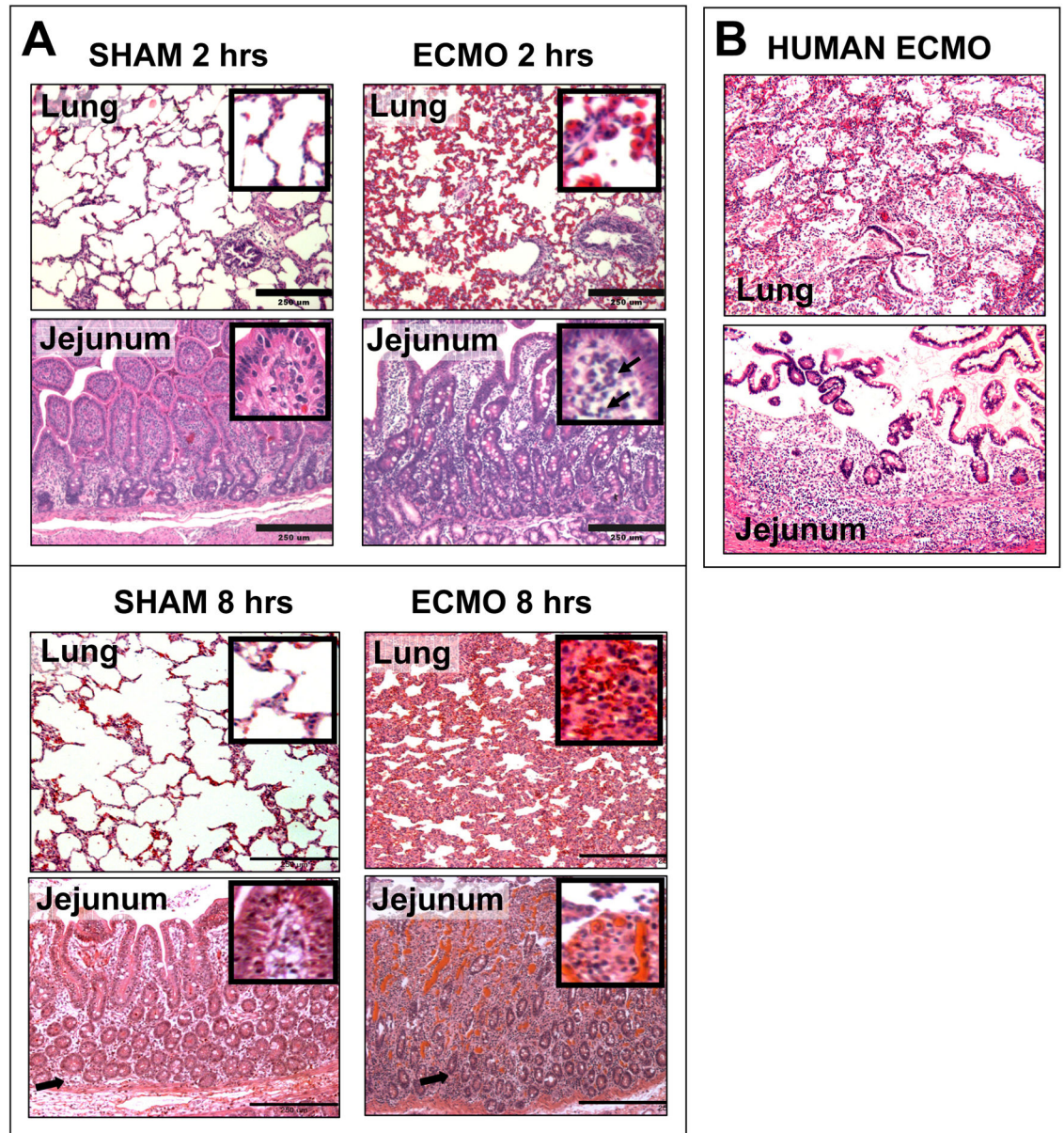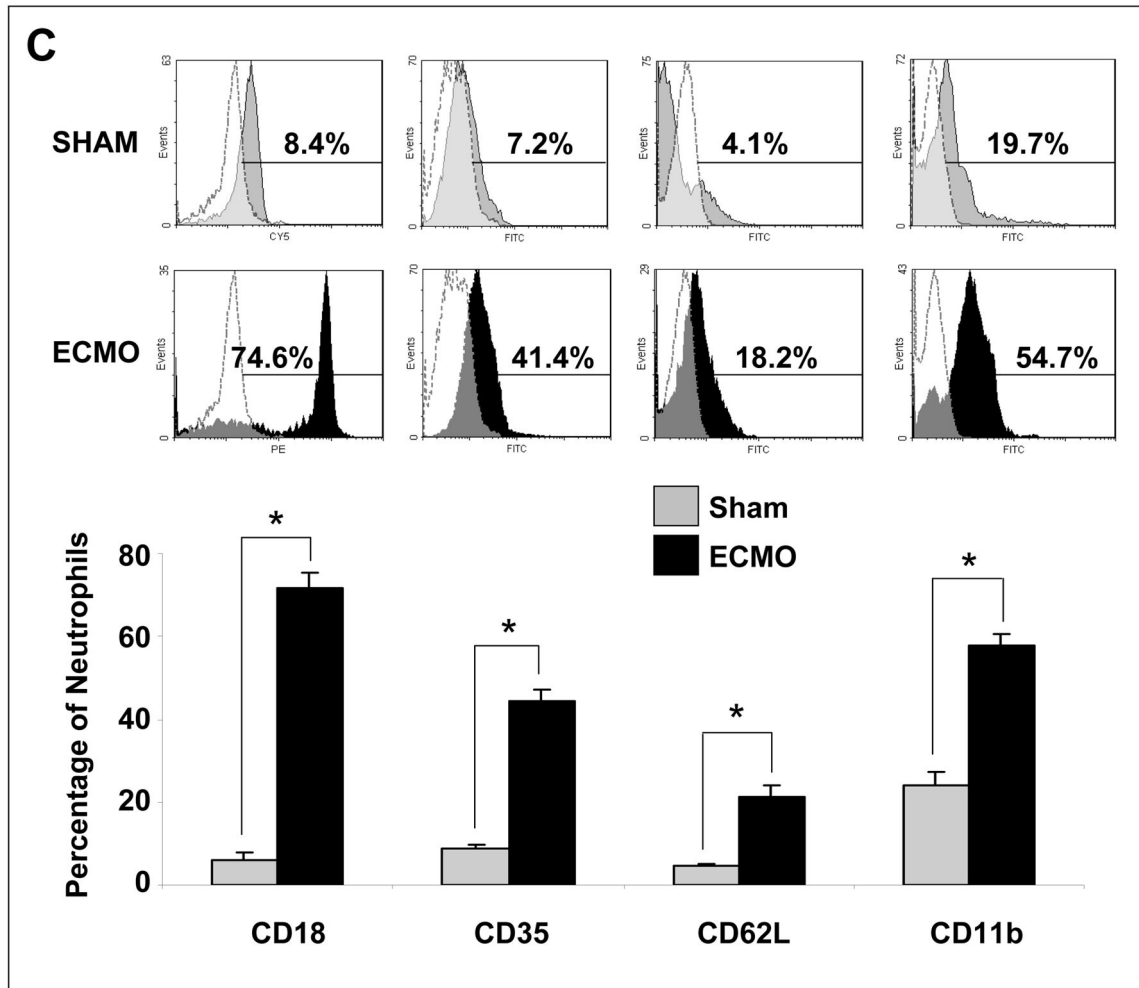
Fig. 1A-B

Fig. 1C

Fig. 1. Histopathological changes of inflammation during ECMO

A. **H&E-stained sections from the lung and the intestine (jejunum) after 2 and 8 hours of ECMO**. *Upper panel:* Histopathological changes after 2 hours of ECMO. Photomicrographs (magnification 100×) highlight the differences between the near-normal alveolar histoarchitecture in sham animals vs. the conspicuous leukocyte infiltration and focal hemorrhages in ECMO. In the intestine, ECMO caused an increase in cellularity in the *lamina propria* (low-magnification), which was due to leukocyte infiltration (higher magnification inset). Data represents n = 3 animals in both groups. *Lower panel:* Histopathological changes after 8 hours of ECMO. Inflammatory changes in the lung became worse with increased leukocyte infiltration, hemorrhages, and septal edema. In the intestine, there was an increase in leukocyte infiltration (black arrows) and focal hemorrhages. The epithelium was disrupted (magnification 100×). Insets shows high-magnification photomicrographs (400×) highlighting the inflammatory changes. Data represents n = 5 animals in both groups. *B.* Photomicrographs of lung and jejunum from human neonates who died during ECMO, showing the marked similarity between inflammatory changes in our porcine model and human tissues. Upper panel shows the

effect of ECMO on the lung, including leukocyte infiltration and alveolar hemorrhages. Lower panel shows marked leukocyte infiltration and disruption of the epithelium in the intestine. Data represent 3 neonates. ***C.* Neutrophil activation during neonatal porcine ECMO.** Representative FACS histograms from sham and ECMO animals drawn after 2 hours of treatment show increased expression of activation markers CD18, CD35, CD62L, and CD11b on circulating neutrophils during ECMO. Bar diagrams shown below the FACS panels summarize the information from an n =5 in both groups. Data were analyzed by the Mann-Whitney *U* test. * indicates a significant difference between ECMO and sham groups, p<0.05.
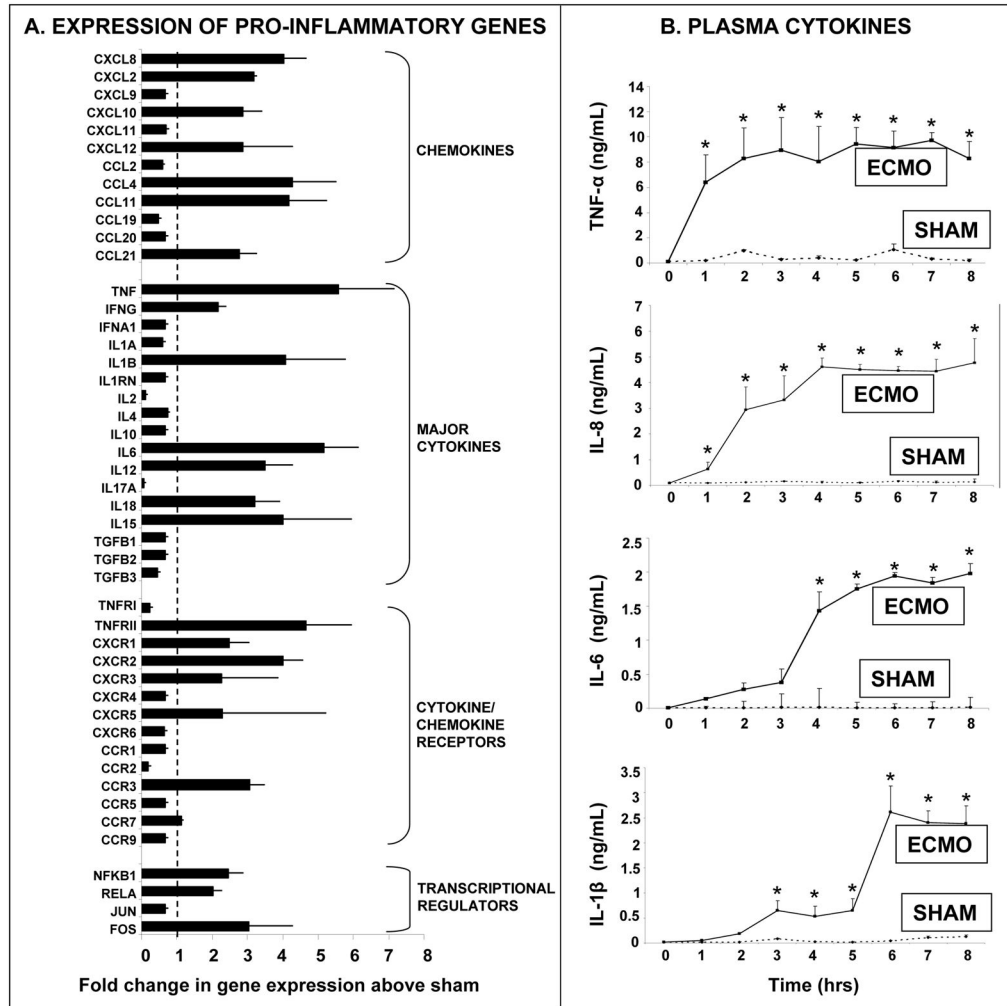
Fig. 2. 'Global' activation of inflammatory mediators in lung tissue during porcine neonatal ECMO

A. Real-time PCR microarray profiles mRNA expression of various pro-inflammatory genes in the lung after 8 hours of ECMO emphasize the 'global' activation of inflammatory mediators during ECMO. Data represent an n =5 animals in both sham and ECMO groups and are depicted as mean ± SEM fold change above sham (dashed line). Gene expression profiles in the intestine were generally similar to those in the lung (not depicted). *B.* Increased plasma concentrations of pro-inflammatory cytokines TNF-α, IL-8/CXCL8, IL-6, and IL-1β as measured by ELISA. Line diagrams depict cytokine concentrations (n=5 animals in sham and ECMO group; means ± SEM). * indicates a significant difference between ECMO and sham groups, p<0.05. Data were analyzed by the repeated measures ANOVA on ranks.
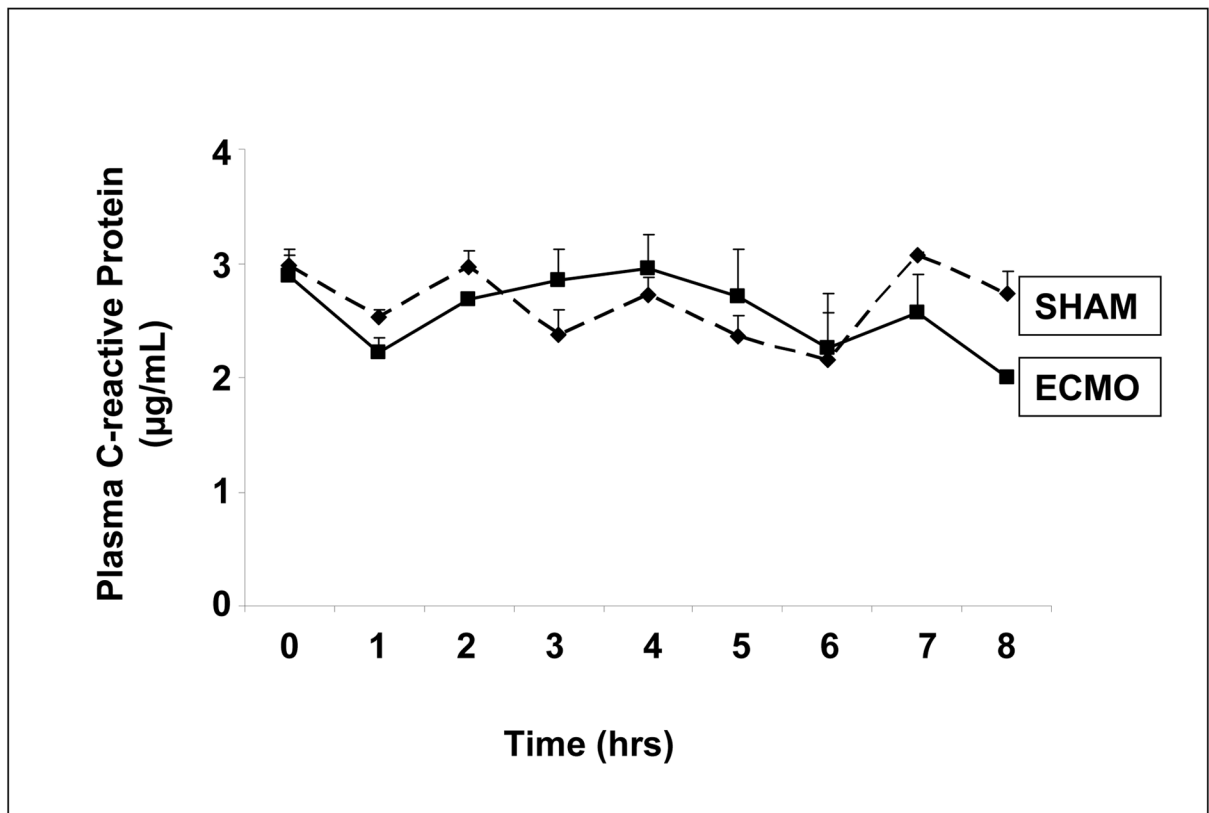
Fig. 3. Onset of systemic inflammatory response during ECMO was not reflected in plasma C-reactive protein concentrations during ECMO

Unlike the marked changes seen in plasma cytokine concentrations, we did not detect significant changes in plasma CRP in the initial 8 hours of ECMO. Other acute phase reactants such as leukocyte counts were also not discriminatory (not depicted). Line diagrams (means ± SEM) summarize information from 5 animals each in ECMO and sham groups. Data were analyzed by the repeated measures ANOVA on ranks.
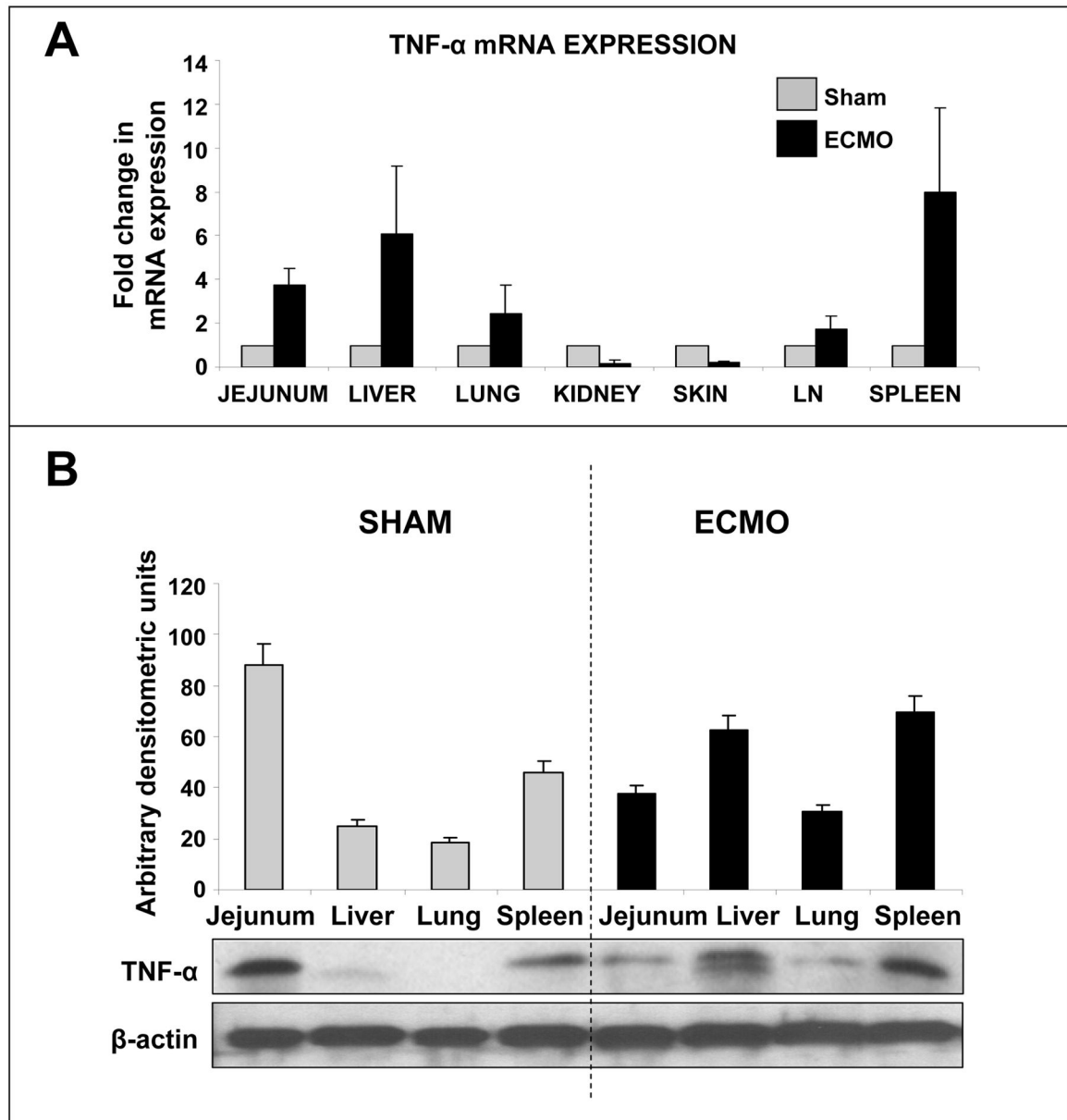
Fig. 4. Rapid rise in plasma TNF-α concentrations during ECMO is not matched by increased synthesis of TNF-α protein in the tissues

We harvested intestine, liver, lung, kidney, skin, mesenteric lymph nodes, and the spleen after 2 hours of ECMO. While the mRNA expression for TNF-α was increased as anticipated, we did not detect an increase in TNF-α protein proportionate to the increase in plasma TNF-α concentrations. *A.* Bar diagrams show the fold-change (means ± SEM) in TNF-α mRNA as measured by real-time PCR after 2 hours of treatment. Data represents an n=3 animals in sham and ECMO groups. *B.* Western blots for porcine TNF-α and β-actin on tissue samples from the intestine, liver, lung, and spleen (the four tissues with the greatest increase in expression of TNF-α mRNA above). Bar diagrams show the densitometric analysis (means ± SEM) of these bands. Data are representative of 3 animals in each group.
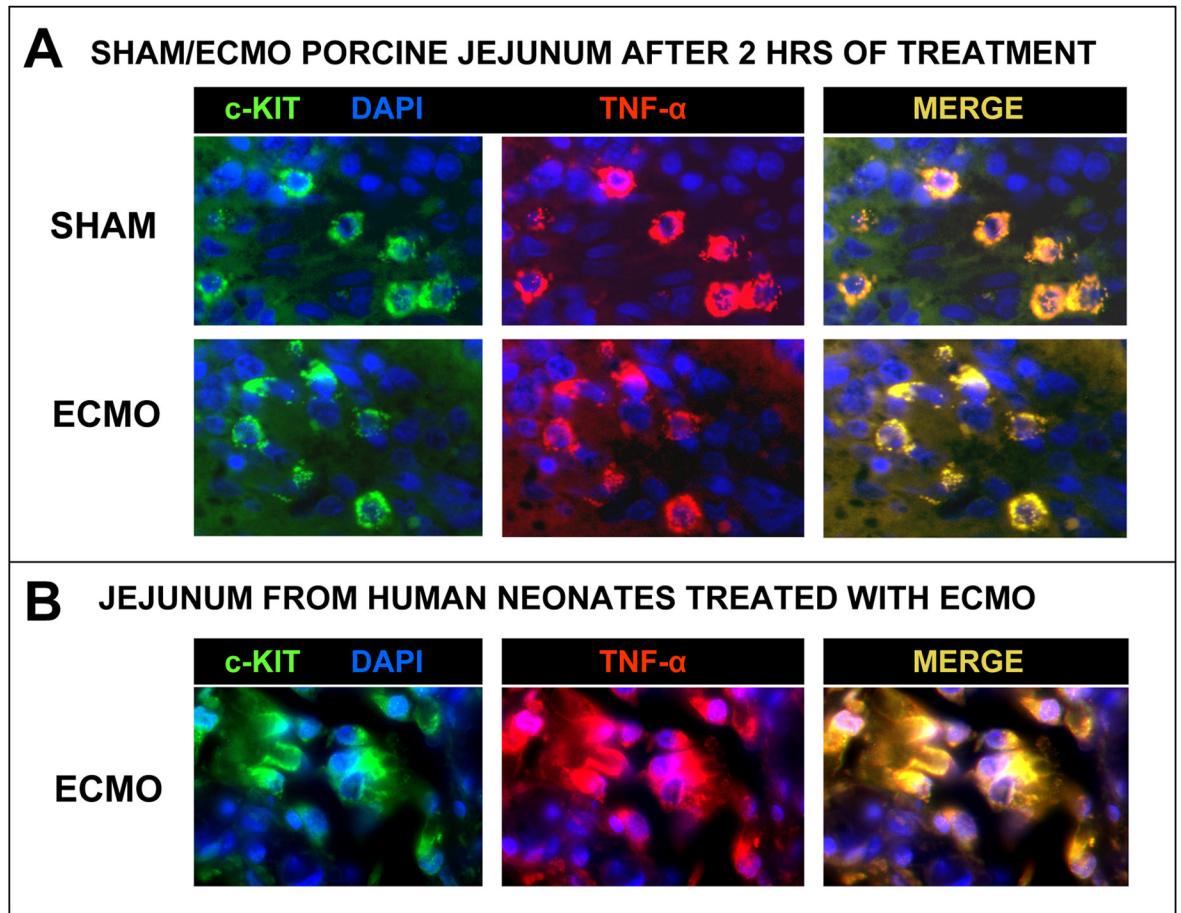
Fig. 5A-B

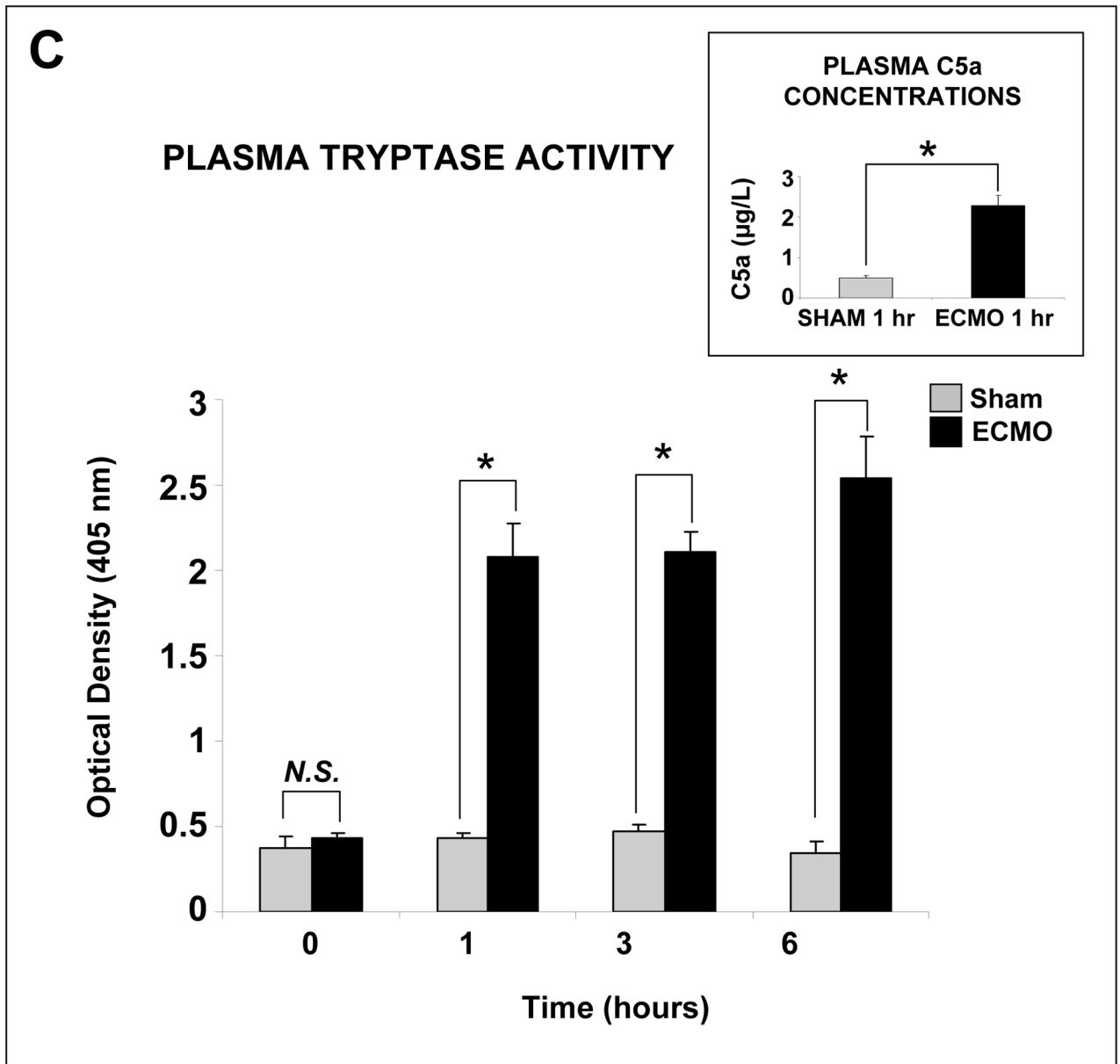**A SHAM/ECMO PORCINE JEJUNUM AFTER 2 HRS OF TREATMENT**

c-KIT DAPI | TNF-α | MERGE

SHAM

ECMO

B JEJUNUM FROM HUMAN NEONATES TREATED WITH ECMO

c-KIT DAPI | TNF-α | MERGE

ECMO

Fig. 5C

Fig. 5.

***A*. Mast cells in the sham/ECMO porcine intestine contain pre-formed TNF-α:**
Immunofluorescence photomicrographs (1000×) from the intestine show strong TNF-α
immunoreactivity in c-kit/CD117^{+} mast cells in both sham animals and after 2 hours of
ECMO. TNF-α immunoreactivity was slightly weaker in ECMO animals than in the sham
group, consistent with our findings of mast cell degranulation during ECMO. Data
representative of 3–5 stained sections from different animals in both sham and ECMO
groups. ***B.*** Similar co-localization of c-kit and TNF-α seen in archived autopsy tissues from
human neonates who died during ECMO. Data represents 3 different neonates. ***C. Porcine***

neonatal ECMO was associated with degranulation of mast cells: Bar diagrams (means ± SEM) show plasma tryptase activity in sham and ECMO animals as a function of time. Plasma tryptase activity was significantly increased after 1 hour of ECMO, indicating that ECMO was associated with mast cell degranulation. Data summarize information from an n =5 animals in both sham and ECMO groups. Statistical comparisons were made by repeated measures ANOVA on ranks. * indicates a significant difference between ECMO and sham groups, *p*<0.05. *Inset:* Bar diagram (means ± SEM) shows that plasma samples after 1 hour of ECMO contained high levels of C5a, a potent mast cell secretagogue released during activation of the complement pathway. Data were analyzed by the Mann-Whitney *U* test. * indicates a significant difference between ECMO and sham groups, p<0.05.